A&A manuscript no.
(will be inserted by hand later)

Your thesaurus codes are:
03(03.20.7,08.06.3)

ASTRONOMY
AND
ASTROPHYSICS
1.2.2008

Research Note : A critique of disentangling as a method of deriving spectroscopic orbits

R.I. Hynes and P.F.L. Maxted ⋆

Astronomy Centre, University of Sussex, Falmer, Brighton, BN1 9QH, England

Received ; accepted

Abstract. Multiple sets of synthetic spectra of OB-binary stars are used to test the suitability of disentangling for deriving accurate spectroscopic orbits. Given a set of spectra with broad phase coverage and sufficient total integration time (almost independent of the number of spectra), it appears that disentangling yields accurate and reliable semi-amplitudes of the spectroscopic orbits (other parameters being fixed). Methods for estimating the uncertainties on the derived semi-amplitudes are investigated.

Key words: stars: fundamental parameters – techniques: radial velocities

1. Introduction

The disentangling technique was first presented by Simon & Sturm (1994, hereafter SS94) and applied to the early B-type binary, V453 Cyg. It has subsequently been used on the O-type systems DH Cep (Sturm & Simon 1994) and Y Cyg (Simon et al. 1994). The original motivation for the method was that it enabled the separation of closely blended spectra, which were then suitable for quantitative analysis. Accurate separation of the spectra requires accurate parameters for the spectroscopic orbit. Those parameters not fixed by other information can, in principal, be determined by finding the values of these free parameters that minimize the residual of the fit to the observed spectra when the separated spectra are recombined.

In this research note we summarize the results of Hynes (1996), in which multiple sets of synthetic spectra were used to investigate whether disentangling is a viable method for determining accurate spectroscopic orbits for a selection of OB eclipsing binary stars.

Send offprint requests to: R.I. Hynes [Email: rih@star.cpes.susx.ac.uk]

⋆ *Present address:* Astronomy Group, University of Southampton, Highfield, Southampton, SO17 1BJ, England

2. The synthetic data

The synthetic binary star spectra are based on a grid of single star spectra kindly provided by Dr C.S. Jeffrey (1996). These cover the spectral range 3600-5000 Å. Each component spectrum was obtained by linear interpolation on the single star grid using the best estimates of $T_{\rm eff}$ and $\log g$, followed by convolution with the appropriate rotational broadening profile. A Doppler shift was then applied to each component based on the adopted spectroscopic orbit and the phase desired and the two shifted spectra were added according to luminosity ratio. Poisson noise was applied to the spectra to produce a realistic signal-to-noise ratio (S/N) (typically S/N=100–200). Ten data sets (each of 15–20 spectra) were generated for each case studied, with phases randomly chosen from a uniform distribution excluding eclipses. Parameters of the systems discussed here are given in Table 1.

For eclipsing systems parameters other than the semi-amplitudes of the spectroscopic orbit (K_1 and K_2) can usually be determined from photometric data. We can therefore estimate optimum values of K_1 and K_2 for each of the ten synthetic data sets using a robust grid searching method. Briefly, the residual, r is calculated for a range of K_1 and K_2 (using our own implementation of SS94's algorithm), using successively finer grids centered on the maximum of the previous grid. The mean difference between the ten resulting K_1, K_2 values and the adopted values indicates the reliability of the method (i.e. this is a test for systematic errors) and the population standard deviation of the ten sets measures its accuracy.

3. Phase distribution

Existing data sets for binary stars are often concentrated around phases near quadrature to minimize problems with blending inherent with established techniques for measuring radial velocities. This is not the best approach to take

Table 1. Adopted parameters of the systems studied together with mean velocities (and errors on this mean) derived by disentangling 10 sets each of 20 synthetic spectra. The final column shows the population standard deviation of the 10 sets and is a measure of the intrinsic scatter of the method.

	L_2/L_1	$v \sin i$ (km/s)	K(km s^{-1}) Adopted	K(km s^{-1}) Derived	Std. dev. (km/s)
A	0.885	165	262.3	262.02±0.17	1.0
		165	278.0	278.12±0.37	1.3
B	0.875	100	235.0	235.08±0.47	1.4
		100	245.0	245.04±0.29	0.9
C	1.156	165	223.0	223.24±0.27	0.8
		200	205.0	204.99±0.26	0.8
D	0.195	165	135.0	135.09±0.17	0.5
		140	190.0	189.83±0.95	2.8
E	0.753	85	145.1	145.08±0.08	0.2
		85	145.8	145.78±0.16	0.5
F	0.868	200	100.0	102.45±1.33	4.8
		200	110.0	108.02±1.34	4.6

with the disentangling procedure. It is clear from the way the equations are set up that the system is best conditioned if the phases cover the full velocity range. This is confirmed by numerical tests (Hynes 1996). Thus it appears that, in contrast to other techniques, the disentangling process will work best when given as broad a phase coverage as possible. This will often be to the observer's advantage.

4. Integration time

We next consider the effects of varying the number of spectra obtained and the duration of each exposure. Both of these can be thought of as varying the total integration time on the target. The combinations chosen are listed in Table 2, together with the resulting uncertainties in deduced parameters, again, for star C. They are plotted in Fig. 1 as a function of total integration time for the primary velocity; similar curves are obtained for K_2. Two power law best fits are plotted; one for variations in number of spectra and the other for variations in exposure time.

It is clear from this figure that there is no significant difference between the two curves i.e. it matters little whether we change the number of spectra obtained or the exposure time of each; it is the *total* exposure time that matters.

5. Accuracy and reliability of the derived orbits

In Table 1 we show the adopted K_1, K_2 values and the mean deduced values derived from 10 sets of synthetic spectra. All the systems studied, with the exception of star F, show no systematic difference between the adopted and deduced K_1, K_2 values i.e. disentangling yields reliable orbital parameters for systems with $v \sin i \lesssim K$. The accuracy of disentangling is estimated from the standard deviation of K_1, K_2 between the 10 sets (Table 1, final column). Accuracies $\sim 1\%$ are found with the exception of star F and star D, presumably due to the high rotational velocity and extreme luminosity ratio, respectively. We also looked at the effect of rectification errors $\sim 5\%$ on the accuracy and reliability of deduced K_1, K_2 values but found no significant effect.

Table 2. Effect of varying the number of spectra and the integration time for Star C.

Number of spectra	Exposure time (s)	$\sigma(K_1)$ (km s^{-1})	$\sigma(K_2)$ (km s^{-1})
20	600	0.5	0.8
15	600	0.7	0.7
10	600	1.9	1.0
5	600	3.0	2.0
20	600	0.5	0.8
20	300	1.1	1.2
20	150	1.7	1.6
20	75	4.3	4.6

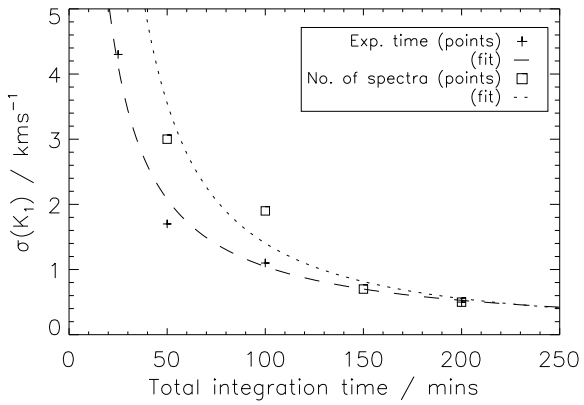

Fig. 1. The effects of varying the exposure time and number of spectra on the uncertainty in the deduced primary semi-amplitude, K_1, Star C. Similar results are obtained for K_2.

6. Estimation of errors

In practice, given a single real data set, we require some method to estimate the accuracy of the K_1, K_2 values derived from disentangling. In this section we test two proposed methods.

6.1. Curvature analysis

As outlined by SS94 and elaborated by Sturm (1994), we can estimate the uncertainties in the derived parameters by converting r to χ^2 using the mean S/N of the observed spectra. The curvature of the χ^2 surface (as a function of the unknown parameters) then yields the uncertainties in the free parameters. The most general method of obtaining confidence intervals from this surface is to construct a contour of constant χ^2, defined by $\chi^2 = \chi^2_{\rm min} + \Delta\chi^2$ and *project* this onto the K_1 and K_2 axes. For the 1σ, two parameter case $\Delta\chi^2 = 2.3$. This assumes a normal distribution of errors which is a good approximation for Poisson noise in the high signal-to-noise limit.

We determined this contour for star E using 10 sets of 20 spectra. The confidence limits on K_1 and K_2 are shown in Table 3. While the deduced uncertainties for K_1 are satisfactory, those for K_2 are somewhat low. This is not unique to this data set – it is a common problem.

Table 3. 1σ confidence limits from the projection of the $\chi^2 = \chi^2_{\rm min} + 2.3$ contour for star E. The population standard deviations between the data sets in this table are 0.25 for K_1 and 0.51 for K_2.

Data set	K_1 ($\rm km\,s^{-1}$)	K_2 ($\rm km\,s^{-1}$)
1	144.8 ± 0.2	145.3 ± 0.4
2	145.0 ± 0.3	145.6 ± 0.4
3	145.1 ± 0.2	145.8 ± 0.4
4	144.9 ± 0.3	145.2 ± 0.4
5	145.1 ± 0.3	146.9 ± 0.3
6	145.5 ± 0.3	145.6 ± 0.3
7	145.2 ± 0.3	145.7 ± 0.3
8	144.7 ± 0.3	145.7 ± 0.6
9	145.4 ± 0.3	145.6 ± 0.4
10	145.1 ± 0.2	146.4 ± 0.4

This is not quite the approach taken by SS94 who instead measure the curvature of the surface at the minimum, represented by the curvature matrix, Γ. The confidence intervals, δK_i, are then given by $\delta K_i = \pm\sqrt{\Delta\chi^2}\sqrt{(\Gamma^{-1})_{ii}}$ (Sturm 1994, Press et al. 1992). We determine the curvature numerically using the data from the final grid for which points are separated by $0.1\,\rm km\,s^{-1}$, which is similar to the expected uncertainty i.e. a suitable value for determination of the curvature. Provided that the surface is smooth, the resulting uncertainties are comparable to those obtained by projection of the confidence region.

6.2. Multiple spectra method

This study was undertaken in preparation for observations using an echelle spectrograph. We therefore decided to investigate whether the standard deviation of the results obtain with different orders of the echellogram would produce reliable uncertainties. We decided upon a simplistic approach, with each order weighted equally. This will degrade the results somewhat, but has the advantage that it does not involve estimating the error from a single order and is therefore independent of methods using the curvature matrix. The spectral range of our synthetic spectra was equivalent to only 4 echelle orders. For the specific case of star E, Table 4 shows that the results obtained by dividing spectra into four sections, each analyzed independently (note that this used a different data run to that in Table 3, so the choice of random phases and the noise will be different). On average, this is an unbiased estimate of uncertainties but the low number of "independent trials" results in poor estimates of the uncertainty in an individual case.

Table 4. Results of disentangling ten synthetic data sets in four separate segments. The population standard deviations between the data sets in this table are 0.4 for K_1 and 0.7 for K_2. Those obtained by disentangling the whole spectra were 0.25 for K_1 and 0.48 for K_2.

Data set	K_1 ($\rm km\,s^{-1}$)	K_2 ($\rm km\,s^{-1}$)
1	145.0 ± 0.3	145.6 ± 0.6
2	145.0 ± 0.3	145.3 ± 1.3
3	145.6 ± 0.4	147.0 ± 1.3
4	144.5 ± 0.2	146.3 ± 0.7
5	145.4 ± 0.3	145.9 ± 0.9
6	144.7 ± 0.2	146.1 ± 0.8
7	145.4 ± 0.3	147.4 ± 1.4
8	145.4 ± 0.2	145.6 ± 0.4
9	145.4 ± 0.5	146.5 ± 0.6
10	145.1 ± 0.3	145.8 ± 0.6

7. Discussion

Our experience with disentangling has led us to be cautious about uncertainties determined from the curvature of χ^2 space near its minimum. These rely on several assumptions which may not be valid in the case of disentangling. For example, it is not clear that the disentangling process is strictly equivalent to model-fitting by least squares minimization and that we can treat it as a two-parameter (i.e. K_1 and K_2) problem. The disentangling procedure simultaneously fits both separated component spectra and the radial-velocity amplitudes; in effect each

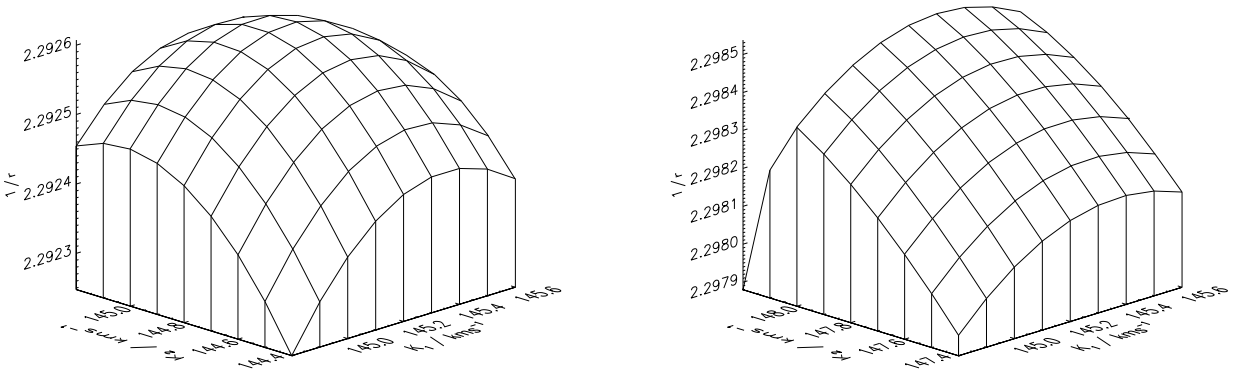

Fig. 2. Two grids resulting from disentangling synthetic spectra of LZ Cen differing only in their random elements.

pixel of each separated spectrum is a parameter to be fitted. In applying curvature analysis as above we are assuming that the separated spectra are simply "nuisance parameters" and can be ignored in the error analysis. This may seem a reasonable assumption but the fact that curvature analysis consistently gets the relative errors on K_1 and K_2 wrong (Section 6.1) indicates that the rôle of the separated spectra may be more subtle.

Statistical subtleties aside, a more pragmatic reason for caution is shown in Fig. 2. Two grids are shown for two synthetic data sets of the same star that differ only in their noise and phase distribution (which are similar). One grid shows a "ridge" near the minimum, a feature that was commonly seen in these grids. The uncertainties derived from the curvature of such a surface are clearly unreliable. In this case, constructing a surface of constant χ^2 would be more appropriate. In surfaces derived from real spectra, even more complex structure can sometimes be seen, for example multiple maxima or a series of parallel ridges. Such effects will further complicate the analysis.

The multiple spectra method appears to give unbiased estimates of the uncertainties but requires more independent spectral sections showing useful spectral lines than are seen in early-type stars. It might well be applicable to late-type stars where even small spectral regions contain a large number of features.

In attempting to analyze the accuracy of the procedure with synthetic data sets we must consider how well we reproduce the characteristics of real data. One issue is that the phase sampling achieved is likely to be less than ideal. We have attempted to mimic this by choosing random phases with no extra constraints (for example we do not impose any restriction on how close in phase two observations can be – real observations spread over several nights could give duplicate phasing). The sharp ridges commented on above may be one manifestation of poor sampling.

Another way in which real data will differ is that the noise distribution is unlikely to be the idealized uncorrelated Poisson noise assumed in this work, e.g. interpolating spectra onto a logarithmic grid is known to introduce a short scale autocorrelation into the noise, which can lead to a "rippling" on the residual surfaces. Other effects, such as cosmic ray events and wavelength calibration errors may also lead to noticable distortions of the surfaces which must be identified and accounted for. Numerical simulations of the type discussed in this paper will be a valuable tool in investigating these issues. For real data however, we will not have the luxury of obtaining multiple duplicate data sets and comparing them. The rôle of simulated multiple data sets is then to give us insight into the reliability of methods such as curvature analysis.

Acknowledgements. R. Hynes was supported by a PPARC Advanced Course Studentship. The authors would like to thank Simon Jeffery for his synthetic single star spectra and Martin Hendry for helpful discussion on matters statistical. P. Maxted would like to thank Klaus Simon for his help and advice.

References

Hynes, R.I. 1996, M.Sc. Thesis, University of Sussex
Jeffrey, C.S. 1996, priv. comm.
Press, W.H., Teukolsky, S.A., Vetterling, W.T., Flannery, B.P. 1992, Numerical Recipes in FORTRAN, 2nd Edn., CUP, Cambridge 1992
Simon, K.P., Sturm, E. 1994, A&A, 281, 286
Simon, K.P., Sturm, E., Fiedler, A. 1994, A&A, 292, 507
Sturm, E. 1994, Ph.D. Thesis
Sturm, E., Simon, K.P. 1994, A&A, 282, 93

This article was processed by the author using Springer-Verlag LaTeX A&A style file *L-AA* version 3.